

Sr in coccoliths of *Scyphosphaera apsteinii*: partitioning behavior and role in coccolith morphogenesis

Erin M. Meyer^a, Gerald Langer^b, Colin Brownlee^{b,c}, Glen L. Wheeler^b & Alison R. Taylor^a

^aDepartment of Biology and Marine Biology, University of North Carolina Wilmington, Wilmington, NC, 28403, USA.

^bMarine Biological Association, The Laboratory, Citadel Hill, Plymouth, Devon PL1 2PB, UK.

^cSchool of Ocean and Earth Science, University of Southampton, Southampton, SO14 3ZH, UK.

Correspondence:

Alison R. Taylor - taylora@uncw.edu, corresponding author.

Erin M. Meyer - emm5468@uncw.edu

Gerald Langer – gerlan@mba.ac.uk

Abstract

Coccolithophores are important contributors to global calcium carbonate through their species-specific production of calcite coccoliths. Nannofossil coccolith calcite remains an important tool for paleoreconstructions through geochemical analysis of isotopic and trace element incorporation including Sr, which is a potential indicator of past surface ocean temperature and productivity. *Scyphosphaera apsteinii* (Zygodiscales) exhibits an unusually high Sr/Ca ratio and correspondingly high partitioning coefficient ($D_{Sr} = 2.5$) in their two morphologically distinct types of coccoliths. Whether or not this reflects mechanistic differences in calcification compared to other coccolithophores is unknown. We therefore examined the possible role of Sr in *S. apsteinii* calcification by growing cells in deplete, ambient, and higher than ambient Sr conditions (between 0.33 - 140 mmol/mol Sr/Ca). The effects on growth, quantum efficiency of photosystem II (Fv/Fm), coccolith morphology, and calcite D_{Sr} were evaluated. No effect on *S. apsteinii* growth rate or Fv/Fm was observed when cells were grown in Sr/Ca between 0.33-36 mmol/mol. However, at 72 mmol/mol Sr/Ca growth rate was significantly reduced, although Fv/Fm was unaffected. At 140 mmol/mol cultures failed to grow. Reducing the Sr/Ca from ambient (9 mmol/mol) did not significantly alter the frequency of malformed and aberrant muraliths and lopadoliths, but at higher than ambient Sr/Ca conditions coccolith morphology was significantly disrupted. This implies that Sr is not a critical determining factor in normal coccolith calcite morphology in this dimorphic species. Using electron dispersive spectroscopy (EDS) we observed an increase in [Sr] and decrease in D_{Sr} of coccoliths as the Sr/Ca of the growth medium increased. Interestingly, muraliths had significantly lower Sr/Ca than lopadoliths at ambient and elevated [Sr], and lopadolith tips had lower Sr than bases in ambient conditions. In summary, the Sr fractionation behavior of *S. apsteinii* is unusual because of an overall high D_{Sr} , and an inter- and intra-coccolith variability in

Sr/Ca. We hypothesize that differential Sr-and Ca-binding capacity of coccolith associated polysaccharides may account for the unusual Sr fractionation of this species which can explain all observations made in this study.

1.0 Introduction

Coccolithophores are unicellular marine algae that produce CaCO_3 plates (coccoliths) intracellularly that are secreted onto the cell surface where they collectively form the calcite coccosphere (Young et al., 1999). Coccolithophores contribute roughly half of global CaCO_3 production, producing $\sim 1 - 1.42 \text{ Gt C yr}^{-1}$ (Daniels et al., 2018; Hopkins and Balch, 2018; Milliman, 1993). Therefore, coccolithophores have a significant impact on ocean biogeochemical cycles through calcification, photosynthesis, and ultimately carbon export (Balch, 2018; Krumhardt et al., 2017; Taylor et al., 2017). Nannofossil coccolith calcite is widely used in micropaleontology, biostratigraphy, and for paleo-reconstructions of ocean ecosystem dynamics (Flores et al., 1997; Saavedra-Pellitero et al., 2017; Stoll et al., 2007a; Stoll et al., 2007b; Young et al., 2014). This is partly due to their distinct morphologies, but also because stable isotope and cation fractionation in coccolith calcite provides tools that can aid paleoreconstructions of oceanic conditions at the time of precipitation.

Past studies have found detectable amounts of strontium (Sr) in coccoliths (Hermoso et al., 2017; Rickaby et al., 2002; Stoll et al., 2002b), and $^{88/86}\text{Sr}$ isotope ratios (seawater:calcite) have been used to model past seawater temperature, Sr cycling, and carbonate chemistry (Muller et al., 2018). Calcite Sr/Ca ratios have also been examined in relation to coccolithophore growth and calcification rates as a measure of ocean productivity. Stoll et al. (2007b) used coccoliths from sediment traps to determine species-specific Sr/Ca ratios, which could then be used to estimate seasonal fluxes of CaCO_3 export. Rickaby et al. (2002) found a positive relationship between growth rate and the Sr incorporation for *Emiliania huxleyi* grown under nitrogen

limitation. Sr incorporation into coccoliths also increased with increased rates of calcification and carbon fixation (Rickaby et al., 2002). However, light induced changes in growth- and calcification rate did not affect Sr partitioning (Langer et al., 2006; Stoll et al., 2002a; Stoll et al., 2002b). Therefore growth and calcification rate per se do not influence Sr partitioning, but some physiological processes altered by nitrogen limitation do (Langer et al., 2006). Through understanding the relationship between Sr incorporation and carbon-specific growth rate, Rickaby et al. (2002) suggested Sr/Ca ratios and ϵ_p (the difference in $\delta^{13}\text{C}$ between dissolved inorganic carbon and organic matter) in coccolithophores could be used as a potential proxy for past surface $p\text{CO}_2$ levels. Variations in cation incorporation can also suggest evolutionary links between extinct and extant coccolithophore species. Based on lower Sr/Ca ratios, Sucheras-Marx et al. (2016) inferred that the mid-Jurassic *Watznaueria britannica* might have been adapted for oligotrophic waters, with slower growth rates than modern equivalent species.

Coccolithophores require one of the highest Ca^{2+} fluxes across the plasma membrane in order to sustain calcification (Brownlee and Taylor, 2004; Brownlee et al., 2015; Taylor et al., 2017), and have multiple modes of Ca^{2+} selective transport both into the cell and to various organelles and compartments (Hermoso, 2014; Mackinder et al., 2010; Marsh, 2003; Outka and Williams, 1971). Because Sr^{2+} has a similar electron configuration and chemical properties to Ca^{2+} , it can potentially enter the cell through Ca^{2+} transporter proteins or channels with a relatively high Sr permeability. Indeed, Sr^{2+} has been used as Ca^{2+} analogue to trace the Ca^{2+} transport pathway in *E. huxleyi* (Gal et al., 2017). Multiple studies have calculated partitioning coefficients (D_{Sr}) from coccolith Sr/Ca ratios (Hermoso et al., 2017; Langer et al., 2006; Stevenson et al., 2014; Stoll et al., 2007b; Sun et al., 2018) resulting in D_{Sr} values varying between 0.02 – 0.6 for various coccolithophore species including *E. huxleyi*, *Gephyrocapsa*

oceanica, and *Coccolithus pelagicus*. *Scyphosphaera apsteinii* is notable for its massive barrel-like lopadoliths and ovoid muroliths that have an unusually high Sr/Ca ratio of 22.1 mmol/mol (Drescher et al., 2012; Hermoso et al., 2017). The resulting D_{Sr} of 2.5 (Hermoso et al., 2017), is an order of magnitude greater than other extant species, implying mechanistic differences in calcite production in *S. apsteinii* that leads to increased Sr/Ca at the site of calcification and the coccolith. One such mechanistic difference could be that CAP functionality in *S. apsteinii* requires unusually high Sr levels in the coccolith vesicle. It was shown that CAP functionality depends on a certain cation composition of the calcifying fluid (Henriksen and Stipp, 2009). We hypothesize that the high Sr/Ca of *S. apsteinii* coccoliths is required for normal morphogenesis, either directly in the calcite lattice or indirectly through an association with CAP. To test this hypothesis we grew *S. apsteinii* in Aquil media containing a range of Sr concentrations (3.3 -720 μ M, for reference, normal seawater has 90 μ M Sr, De Villiers, 1999), and analyzed coccolith morphology and Sr/Ca ratios.

Based on the idea that Sr^{2+} takes the same cellular route as Ca^{2+} (see above), a conceptual model describes Sr partitioning in coccolithophores as a steady state scenario (Langer et al., 2006). In its simplest form this model predicts an even distribution of Sr in the coccolith. Indeed, previous studies on different species suggest an even distribution of Sr (Grovenor et al., 2006; Prentice et al., 2014; Sucheras-Marx et al., 2016). However, the investigated species display coccolithophore-typical Sr partitioning behavior, i.e. have a much lower Sr/Ca than *S. apsteinii*. We hypothesize that the atypical Sr partitioning of *S. apsteinii* might include non-uniform Sr distribution within the coccoliths, and differences in Sr/Ca between the morphologically distinct lopadoliths and muroliths. To test these hypotheses, we performed analytical scanning electron microscopy (SEM) combined with electron dispersive spectroscopy (EDS).

2.0 Methods

2.1 Maintenance of algal cultures, experimental media, and growth conditions

S.apsteinii strain RCC 1456 was obtained from the Roscoff Culture Collection, France. Batch cultures were maintained in sterile 40 mL polystyrene flasks in a modified L1 medium (LH; Fowler et al., 2015) comprising autoclaved and filter sterilized Gulf Stream seawater, amended with LH nutrients and vitamins. The [Sr] of the seawater was 95.4 μM Sr as determined using ICP-MS, which is expected for seawater. Experimental cultures were grown in Aquil media, modified from (Kester et al., 1967) by adding f/8 metals, f/8 vitamins, 1 mL/L of sterilized Gulf Stream seawater, and modifying the following nutrients: 64 μM NO_2^- , 4 μM PO_4^{3-} , and 10 nM SeO_2 . The [Sr] of the Aquil medium was 3.3 μM as determined using ICP-MS. A 1M $\text{SrCl}_2 \cdot 6\text{H}_2\text{O}$ stock solution (Puratronic, 99.9965%, 10877, Alfa Aesar) was used for amending the [Sr] of the Aquil media from 3.3 (no added Sr), to 90, 360, and 720 μM Sr. The cells were acclimated for at least 8 generations in the corresponding Aquil/Sr medium to ensure all attached coccoliths were produced in the presence of the treatment [Sr]. All cultures were maintained at 15°C on a 14:10 h light:dark cycle, at approximately 100 $\mu\text{mol m}^{-2} \text{ s}^{-1}$ with sub-culturing at mid-late exponential growth phase.

Cultures acclimated to each [Sr] treatment were harvested at mid-exponential growth and used to establish four replicate experimental flasks with a starting density of $\sim 1 \times 10^3$ cells mL^{-1} . Cell counts were recorded over 10 d using a Sedgewick-Rafter chamber with a minimum of 300 cells counted per sample. Cell densities were plotted versus time and growth rate (μ) was calculated from exponential regression including all data-points till harvest day (day 10).

The quantum yield of photosystem II (F_v/F_m) was estimated using an AquaPen AP 100 fluorometer (PSI, Drasov, Czech Republic). Approximately 1.5 mL of sample from each flask was placed in a cuvette and dark-adapted at room temperature for 15 min prior to measurements. An average of 3 measurements was taken over 3 min with cuvettes gently inverted to resuspend cells 10 s prior to each measurement.

2.2 SEM and EDS

Mid-exponential *S. apsteinii* cells were used for SEM and EDS analysis. A 1.5 mL aliquot of each replicate culture for each [Sr] treatment was syringe filtered onto 13 mm 0.4 μm Isopore filters [Merck Millipore Ltd.] followed by buffered Nanopure water (1 mM HEPES, pH 8.0) to remove salts. Filters were air-dried and mounted onto an aluminum stub with carbon adhesive tabs before coating with 10 nm Pt/Pd. Samples were analyzed using a FEI Verios 460L SEM equipped with an Oxford Xmax silicon drift EDS detector and AZtec acquisition and analysis software (Oxford Instruments, UK). The primary beam acceleration was 10 kV (EDS and electron backscatter imaging mode) or 2 kV (secondary electron imaging). For EDS, spectra were from 1-2 μm diameter regions of interest collecting for 60 s between 2,000 – 8,000 cps with an average deadtime < 5%. Peaks for major elements of coccoliths were auto-detected and Pt/Pd peaks were eliminated. Standardless quantification was used to estimate atomic % (At%) and weight % (Wt%) compositions of calcite. A power analysis suggested a minimum sample size of 12 was needed to statistically detect an effect size of ≥ 0.15 At% Sr. Therefore, at least 31 spectra were taken for muroliths and at the base and tip of each lopadolith. Wt% values were used to determine Sr/Ca mmol/mol of calcite (Hermoso et al., 2017) which were subsequently used to calculate D_{Sr} (Eq. 2).

$$\text{Eq 1: } \frac{\text{Sr mmol}}{\text{Ca mol}} = 1000 * \frac{\text{Sr [Wt\%]}}{\text{Ca [Wt\%]}} * \frac{\text{Ca MW}}{\text{Sr MW}}$$

$$\text{Eq 2: } D_{\text{Sr}} = \frac{\text{Sr/Ca mineral}}{\text{Sr/Ca medium}}$$

Effects of [Sr] on coccolith morphology were determined by scoring coccoliths from 40 cells for each treatment. Coccoliths were only scored if the majority of the coccolith could be seen. Muroliths were scored into four categories: normal, malformed, incomplete, and aberrant (see Fig 2). Lopadoliths were scored into five categories: normal, malformed (minor malformations commonly seen in control cultures), Type S (incomplete, normal calcite morphology), Type R (longitudinal cleavage in lopadoliths), and Type T (aberrant, completely disorganized calcite; see Fig 2). Scores for each morphometric category are presented as the average of the experimental replicates (n=4).

2.3 Statistics

A one-way ANOVA was completed in SigmaPlot 14.0 to compare differences in morphology between Sr treatments. The data was found to be not normal through a Shapiro-Wilks test, therefore we used a Tukey's pairwise comparison. A t-test was used for comparing growth rates, Sr/Ca mmol/mol, D_{Sr} , and differences in Sr content between muroliths and lopadoliths. The data was found to be not normal through a Shapiro-Wilks test, therefore we used a Mann-Whitney Rank Sum test. Differences between Sr content in lopadolith bases and tips were analyzed using a Student's t-test.

3.0 Results

3.1 Sr effects on physiology and coccolith morphology

There was no significant effect of low Sr on growth rate and photosynthetic physiology (Fig. 1A-B); however, cells grown in 72 mmol/mol Sr/Ca had significantly lower growth rates ($p < 0.01$; Fig1A). Cells grown in 144 mmol/mol Sr/Ca stopped dividing almost immediately after exposure, implying a potential Sr toxicity, and were not further analyzed (data not shown). Average F_v/F_m values ranged from 0.55 – 0.58 and were unaffected by [Sr] over the range 0.33-72 mmol/mol Sr/Ca, indicating there was no overall physiological cell stress due to either lower or higher than ambient Sr (Fig. 1B). The average Sr/Ca in *S. apsteinii* coccolith calcite was three times that of the ambient medium (27.0 ± 10.8 vs 9 mmol/mol; Figure 1C-D). Coccolith calcite Sr/Ca significantly increased with increasing media [Sr] ($p < 0.001$; Fig. 1C-D; Table 1) although the corresponding D_{Sr} decreased with the relationship best described as a second-order polynomial curve ($r^2 = 0.92$; $p < 0.001$; Table 1).

Coccolithogenesis was disrupted when *S. apsteinii* were grown in higher than ambient [Sr], resulting in increased frequency of malformed and aberrant coccoliths (Fig. 2). The 0.33 mmol/mol group had the highest frequency of normal coccoliths ($p < 0.001$) and fewest morphological disruptions to their coccoliths (Fig. 2; Fig. 3), while the 72 mmol/mol group had significantly more Type R ($p < 0.001$) and Type T ($p < 0.05$) lopadolith malformations and aberrant muroliths ($p < 0.001$; Fig. 3; Table 2). Type R coccoliths were seen frequently in response to elevated Sr concentrations, showing jagged edges along the lopadolith tips (Fig. 2; Fig. 3).

3.2 Sr/Ca and D_{Sr} correlates with Sr/Ca of medium and varies between and within coccolith types

When comparing cells grown at ambient [Sr], we observed muroliths had significantly less Sr than lopadoliths (22.9 ± 10.6 and 31.1 ± 9.5 Sr/Ca mmol/mol respectively; $p < 0.001$; Fig.

4). The lower murolith Sr content was consistent among all [Sr] treatments analyzed (Fig. 4; Table 2). Correspondingly, D_{Sr} for muroliths was significantly lower than lopadoliths across all [Sr] treatments ($p < 0.001$; Table 2). The limit of detection for Sr using EDS was determined to be 0.2 Wt% (2.29 mmol/mol). The Sr/Ca values for coccoliths grown in the 0.33 mmol/mol Sr/Ca treatment were clearly much lower than the other treatments, but considered to be below the technical LOD and not reported here, although the technical LOD is indicated on relevant graphs.

Because of the large size of *S. apsteinii* coccoliths, the spatial distribution of Sr in lopadoliths was examined by acquiring EDS estimates of Sr/Ca from base and tip regions of these barrel-like structures. Lopadolith tips had a small but significantly lower Sr incorporation compared to bases in cells grown in ambient [Sr] (28.8 ± 9.87 and 33.6 ± 8.51 Sr/Ca mmol/mol respectively; $p < 0.05$; Fig. 5) although the calculated D_{Sr} values were lower but not significant ($p = 0.05$) between tip and base. The spatial difference in Sr/Ca between base and tip was not significantly different in cells grown at higher than ambient [Sr] (Fig. 4; Table 2).

4.0 Discussion

4.1 Fractionation for Sr in *S. apsteinii*

Our results are consistent with Hermoso et al. (2017) in that there is unusually high Sr/Ca in *S. apsteinii* calcite compared to other species. We also observed an increase in coccolith Sr/Ca and a decrease in D_{Sr} with increasing media Sr concentrations, which is in line with several studies (Hermoso et al., 2017; Payne et al., 2008; Sun et al., 2018). A range of Sr/Ca ratios in coccolithophores has been reported (Prentice et al., 2014; Stoll et al., 2002b; Stoll et al., 2007b) with a trend for small coccolithophores such as *E. huxleyi* and *G. oceanica* significantly

fractionating against Sr, yielding Sr/Ca ratios of ~3 and 1.2 mmol/mol respectively (Hermoso et al., 2017; Stoll et al., 2002a). This relationship appears to also hold true for mixed field samples in which sediments with an abundance of larger species bearing bulky coccoliths such as *Calcidiscus leptoporus* are associated with higher Sr/Ca ratios (between 2 and 2.4 mmol/mol) than sediments dominated by smaller species such as *E.huxleyi* (Stoll and Schrag, 2000). The D_{Sr} in *S.apsteinii* at ambient [Sr] ($D_{Sr} = 3$, this study) is similarly much higher when compared to other species such as *E.huxleyi* (0.1-0.6; Langer et al., 2006; Muller et al., 2018; Rickaby et al., 2002; Stevenson et al., 2014), *G.oceanica* (0.14 – 0.34; Hermoso et al., 2017; Stevenson et al., 2014), and *C. braarudii* (0.31 – 0.43; Muller et al., 2018; Stevenson et al., 2014).

To explain the unusually high Sr/Ca ratio in *S.apsteinii*, Hermoso et al. (2017) proposed a multi-step cellular process whereby Ca^{2+} channels in the plasma membrane fractionate in favor of Sr with additional fractionation for Sr through intracellular Ca^{2+} transport through an unexplained mechanism. A Ca^{2+} return flux from the CV into the cytosol through Ca^{2+} channels is also proposed to fractionate against Sr, further enriching Sr at the site of mineralization. We offer several additional perspectives to interpret the high Sr content observed in *S. apsteinii* coccoliths.

Fractionation of plasmamembrane Ca^{2+} channels for Sr^{2+} as proposed by Hermoso et al. (2017) could explain the high D_{Sr} of *S. apsteinii*. In fact, a higher Sr^{2+} permeability ($Sr^{2+} > Ca^{2+}$) has been demonstrated in animal systems for R- and L-Type Ca^{2+} channels, such as Ca_v 1.3 (Bourinet et al., 1996; Rodriguez-Contreras et al., 2008; Rodriguez-Contreras and Yamoah, 2003). This scenario implies that Ca^{2+} channels in *S. apsteinii* have a different Sr fractionation behavior (i.e. relative permeability) than channels in other coccolithophores studied so far. While this is possible it would have to be a specific feature of the Pontosphaeraceae (or even

Scyphosphaera) because *Helicosphaera carteri* (also a member of the Zygodiscales) displays a fractionation against Sr, similar to the studied Coccolithales and Isochrysidales (Stoll et al., 2007b). As critical data on coccolithophore Ca^{2+} channels is lacking, future work should assess the permeability of these channels to Sr^{2+} . Additionally, using published calcification rates (Gafar et al., 2019), we calculate that *S.apsteinii* exhibit over twice the calcification rate of *E.huxleyi* when normalized to cell surface area ($0.45 \text{ pg}/\mu\text{m}^2/\text{d}$ vs $0.18 \text{ pg}/\mu\text{m}^2/\text{d}$, respectively). Production of large, bulky *S.apsteinii* coccoliths therefore requires over twice the flux of Ca^{2+} per unit membrane surface area than *E.huxleyi*. The higher calcification rates combined with lower cation selectivity for Ca^{2+} transporters could contribute to the increased Sr/Ca relative to seawater in *S.apsteinii* coccoliths.

There are, however, alternative explanations for the high D_{Sr} in *S. apsteinii*. Amorphous calcium carbonate (ACC) favors trace metal (Sr) incorporation into the crystal lattice structure in inorganic systems (Littlewood et al., 2017). Higher than expected Sr incorporation could theoretically be explained if *S. apsteinii* utilizes an ACC precursor phase for calcite precipitation. Although an ACC precursor is used in many biomineralization systems such as in foraminifera and mollusk shell formation (Addadi et al., 2006; De Nooijer et al., 2014), and has been considered as a possible intermediate in coccolithophore calcification (Brownlee et al., 2015), there is no current evidence for its use in coccolithophore biomineralization. Moreover, the hypothesis that *S. apsteinii* uses ACC while other coccolithophores do not, implies species specific differences in calcification mechanisms at a basic level (mode of calcium carbonate precipitation).

A more parsimonious explanation is differences in calcification mechanisms at a higher level, such as species-specific coccolith associated polysaccharides (CAP; Fichtinger-Schepman

et al., 1981; Marsh et al., 2002). CAP play an important role in coccolith morphogenesis, mainly as inhibitors of crystal growth (Borman et al., 1982; Marsh, 1994; Westbroek et al., 1984). An inorganic study found that when using malonic acid to mimic the function of CAP by blocking acute calcite kink sites, *c*-axis elongation occurred as similarly seen in heterococcoliths (Payne et al., 2008). While species-specific CAP are likely playing the same functional role, their precise involvement in determining crystal growth and morphology could be subtly different among species. For example, some CAP influence crystal morphology by site-specific attachment to crystallographic steps (Henriksen et al., 2004), but others might not. *S. apsteinii* have CAP that are known to differ from those of some placolith bearing species, such as *C. braarudii* (Walker et al., 2018a). We propose that the difference in CAP between *S. apsteinii* and other species could contribute to different Sr fractionation behavior in at least three ways: 1) intra coccolith vesicle CAP could alter the vesicle Ca^{2+} concentration needed to achieve super-saturation, which would in turn affect Sr fractionation (Langer et al., 2006). 2) Different CAP might have different Sr binding capacity or requirements, akin to brown algae polysaccharides (Davis et al. 2003), which might influence coccolith vesicle Sr/Ca. Such a mechanism is supported by inorganic experiments in which growing calcite crystals exposed to increasing [malonic acid] resulted in higher Sr incorporation. As this process mimics CAP-Sr interactions, it could explain the variable Sr incorporation seen among coccolithophore species (Payne et al., 2008). 3) Incorporation of CAP itself within coccoliths could introduce an organic phase with an interspecific Sr/Ca. Because different kinds of CAP are used for different (partly morphogenetic) purposes (Marsh, 2000; Walker et al., 2018a), CAP-specific Sr fractionation offers a good explanation for inter as well as intra (see below) specific differences in Sr fractionation. Overall,

we conclude that CAP likely influence Sr fractionation and there are several ways in which this could happen.

4.2 Variable inter- and intra- coccolith Sr fractionation in *S. apsteinii*

The different Sr fractionation between muraliths and lopadoliths, and spatially within lopadoliths, was unexpected. Secondary ion mass spectroscopy analysis of extant and microfossil placolith-bearing species such as *C. braarudii* and *Reticulofenestra bisecta* demonstrates spatially uniform minor element distribution (Grovenor et al., 2006; Prentice et al., 2014; Sucheras-Marx et al., 2016). This is in accordance with the prediction of a conceptual model (in its simplest form) describing Sr fractionation in *E. huxleyi* (Langer et al., 2006). A refined version of the model considers the effect of species-specific CAP-related Sr fractionation but does not consider coccolith type-specific fractionation, let alone intra coccolith variability in CAP influence (Langer et al., 2006). We propose that the model by Langer et al. (2006) is modified to incorporate a non-constant CAP factor within any given species. Applying the concept of a non-constant CAP factor, both coccolith type-specific and intra coccolith position-specific Sr fractionation can be accounted for. We propose that *S. apsteinii* uses different CAP for muralith and lopadolith formation respectively, as well as for lopadolith bases and tips.

Another advantage of the “CAP-hypothesis” is that it can potentially explain why D_{Sr} in *S. apsteinii* decreases with increasing seawater [Sr] (Table 2B): The resulting high coccolith vesicle Sr/Ca could possibly change CAP structure/conformation (Ishii et al., 1999; Kucerka et al., 2008) in such a way that the Ca^{2+} binding capacity of CAP increases (Woodward and Davidson, 1968). This increased Ca^{2+} binding capacity will then increase the vesicle $[Ca^{2+}]$ concentration needed to achieve super-saturation with respect to calcite, which will in turn decrease D_{Sr} (Langer et al. 2006).

4.3 Sr is not required for morphogenesis in *S. apsteinii*

Because coccolith morphology was unaffected in *S. apsteinii* cells grown in a [Sr] that was over 25-fold lower than ambient (0.33 vs 9 mmol/mol), we conclude that Sr is not essential for coccolith morphogenesis of the unusually bulky coccoliths of this species. On the contrary, higher [Sr] resulted in significant disruption of normal crystal morphogenesis as evidenced by a dramatic increase in the number of aberrant coccoliths produced. The lower growth rates for coccolithophores grown in 72 mmol/mol Sr/Ca, and the inability of cells to grow in media [Sr] above this, could be the result of a compromised coccosphere potentially impeding their ability to properly divide. A similar effect was observed in *C. pelagicus* in which calcification was disrupted using three separate approaches; Low Ca^{2+} , the metal chelator 1-hydroxyethane 1,1-diphosphonic acid (HEDP), and the Si analogue Ge (Walker et al., 2018b).

4.4 Why does high Sr/Ca disrupt *S. apsteinii* coccolith morphogenesis?

The increased frequency of Type R malformations in response to the 36 and 72 mmol/mol Sr/Ca treatments suggests the disruptive effect of high Sr on morphology is not purely through inorganic processes (Wasylenki et al., 2005). An inorganic mechanism of Sr-induced disruption would affect the whole coccolith, but Type R malformations are extremely site specific and leave most of the coccolith unaffected. Furthermore it is unlikely that aberrant coccoliths are the result of high Sr interfering with the cytoskeleton otherwise cell division and growth rate would be affected (Durak et al., 2017; Langer et al., 2010), which is not the case at 36 mmol/mol Sr/Ca. Alternatively, as discussed above, CAP profoundly influence coccolith morphology (Borman et al., 1982). CAP bind divalent cations and their morphogenetic function depends on the ionic composition of the fluid (Davis et al., 2003; Grant et al., 1973; Henriksen

and Stipp, 2009). Possibly high Sr/Ca changes CAP structure/conformation (Ishii et al., 1999; Kucerka et al., 2008) which impairs their morphogenetic function (Henriksen and Stipp, 2009).

4.5 Concluding Remarks

S. apsteinii shows a weak Sr fractionation (high D_{Sr}) in their calcite coccoliths that is significantly higher than that of any coccolithophore (extant or extinct) for which Sr/Ca has been determined. Our results show that Sr is not necessary for normal muralith or lopadolith morphogenesis. However, elevated levels of Sr in the medium disrupt coccolith morphogenesis and ultimately cell division likely due to an incomplete coccosphere. We show that *S. apsteinii* fractionates Sr differently between and within coccolith types, suggesting Sr incorporation is not solely governed by a simple steady state Sr- and Ca flux to the CV. A variety of species-specific CAP that regulate morphogenesis may underlie the spatial and morphologically distinct Sr fractionation. Although Sr/Ca in coccoliths has been used to reconstruct past coccolithophore productivity, the coccolithophore Sr/Ca proxy remains poorly understood. Our study implies that inter- and intraspecific organic phases play a critical role in minor element incorporation into coccoliths and therefore need to be considered when developing a mechanistic understanding of proxy relationships.

Acknowledgements

We thank Dr. Jack Pender at Eastern Carolina University for running seawater Sr analysis using ICP-MS. The work was supported by NSF GEO-NERC grant 1638838 to ART and by Natural Environment Research Council grant NE/N011708/1. Analytical electron microscopy was performed in part at 1) Analytical Instrumentation Facility (AIF) at North Carolina State

University, supported by the State of North Carolina and the National Science Foundation (award number ECCS-1542015) and 2) Joint School of Nanoscience and Nanoengineering, a member of the Southeastern Nanotechnology Infrastructure Corridor (SENIC) and National Nanotechnology Coordinated Infrastructure (NNCI), which is supported by the National Science Foundation (Grant ECCS-1542174).

ERC

Tables and Figures

Table 1 *S.apsteinii* murolith (A) and lopadolith (B) morphology in response to Sr. The morphology of coccoliths from 10 cells per replicate flask for each Sr treatment were scored under an SEM. Scores for each morphometric category are presented as the average of the experimental replicated (n = 4). Type S: an incomplete lopadolith with normal calcite morphology. Type R: a lopadolith with longitudinal cleavage. Type T: an aberrant lopadolith with completely disorganized calcite. Significantly more normal coccoliths were scored in the 0.33 mmol/mol Sr/Ca treatment (p < 0.001), while more aberrant muroliths (p < 0.001) and lopadoliths (Type R: p < 0.001; Type T: p < 0.05) were scored in 72 mmol/mol Sr/Ca.

A.

Media Sr/Ca (mmol/mol)	Normal Muroliths [± sd]	Incomplete Muroliths [± sd]	Malformed Muroliths [± sd]	Aberrant Muroliths [± sd]
0.33	51.4 [7.8]	21.3 [8.0]	24.8 [3.8]	2.5 [2.3]
9	44.3 [6.8]	20.3 [2.5]	32.2 [3.2]	3.3 [1.7]
36	40.8 [4.2]	23.5 [1.7]	28.2 [3.2]	7.5 [6.8]
72	16.2 [2.3]	29.0 [9.4]	37.4 [5.3]	17.4 [8.0]

B.

Media Sr/Ca (mmol/mol)	Normal Lopadoliths [± sd]	Malformed Lopadoliths [± sd]	Type S Lopadoliths [± sd]	Type R Lopadoliths [± sd]	Type T Lopadoliths [± sd]
0.33	66.8 [12.7]	11.6 [9.0]	12.3 [3.3]	7.0 [3.4]	2.2 [2.6]
9	46.9 [3.5]	23.0 [4.7]	22.5 [5.5]	7.7 [7.3]	0.0 [0.0]
36	47.4 [12.3]	20.8 [10.1]	18.4 [9.4]	11.4 [3.0]	2.1 [4.2]
72	14.5 [3.3]	18.7 [7.1]	20.0 [3.0]	34.9 [10.4]	11.9 [9.6]

Table 2 Sr incorporation (A) and partitioning coefficients (B) in *S.apsteinii* coccoliths from cells grown under ambient and high external [Sr]. The calcite Sr/Ca mmol/mol ratio represents the amount of Sr relative to Ca in coccolith calcite, which significantly increases with increasing Sr media concentration ($p < 0.02$). The D_{Sr} is the Sr partitioning coefficient which exponentially decreases with increasing Sr media concentration ($p < 0.001$). Note that for the 0.33 mmol/mol Sr/Ca treatment, EDS Sr was below the technical LOD and subsequent values were not determined.

A.

Media Sr/Ca (mmol/mol)	Calcite Sr/Ca (mmol/mol) [± sd]	Murolith Sr/Ca (mmol/mol) [± sd]	Lopadolith Base Sr/Ca (mmol/mol) [± sd]	Lopadolith Tip Sr/Ca (mmol/mol) [± sd]
.33	ND	ND	ND	ND
9	27.0 [10.8]	22.9 [10.6]	33.6 [8.51]	28.8 [9.87]
36	36.8 [18.3]	31.7 [16.7]	45.4 [16.3]	40.7 [19.2]
72	51.3 [27.1]	39.6 [23.4]	62.9 [24.8]	59.9 [23.3]

B.

Media Sr/Ca (mmol/mol)	D _{Sr} [± sd]	Murolith D _{Sr} [± sd]	Lopadolith Base D _{Sr} [± sd]	Lopadolith Tip D _{Sr} [± sd]
0.33	ND	ND	ND	ND
9	3.00 [1.20]	2.54 [1.18]	3.74 [0.95]	3.20 [1.10]
36	1.02 [0.51]	0.88 [0.46]	1.26 [0.45]	1.13 [0.53]
72	0.71 [0.38]	0.55 [0.33]	0.87 [0.34]	0.83 [0.32]

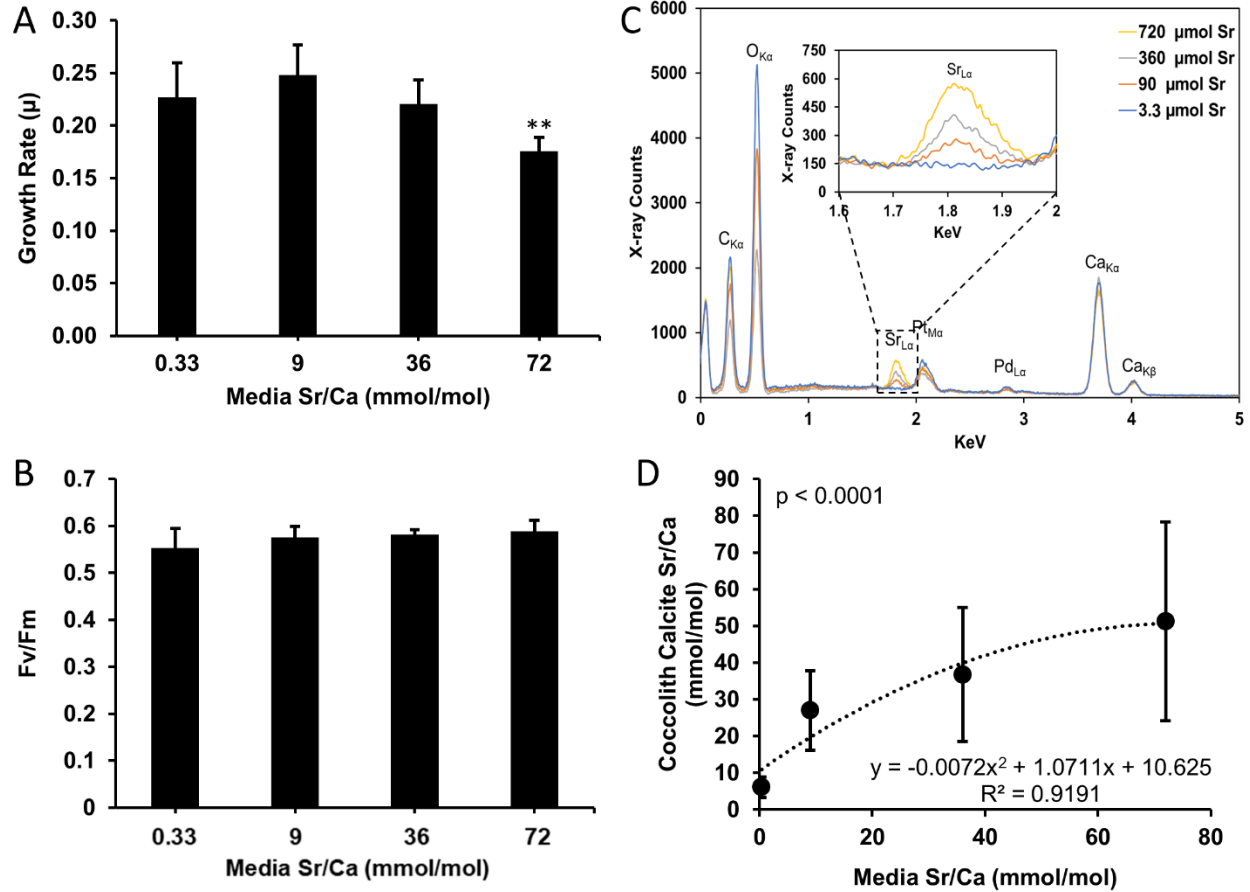


Figure 1. Growth and physiology unaffected by Sr incorporation when grown in deplete and enriched Sr media

(A) Maximum growth rate (μ) of *S. apsteinii* determined over 10 d in deplete, ambient, or enriched Sr treatments (N = 4 independent replicates for each Sr treatment \pm SD). Cells grown in 72 mmol/mol Sr/Ca had a significantly lower growth rate ($p < 0.01$; student's t-test) and cells grown in 142 mmol/mol failed to grow. (B) Quantum yield of photosystem II (F_v/F_m) of dark-adapted *S. apsteinii* cells grown under the same Sr/Ca treatments showed no significant difference (N = 4 independent replicates for all Sr treatments \pm SD, student's t-test). (C) Example EDS spectra showing increased Sr incorporation for *S. apsteinii* coccoliths grown in deplete, ambient, and enriched Sr. Inset: detail of the EDS spectra showing Sr peaks among Sr treatments. (D) Average Sr/Ca (\pm SD) of *S. apsteinii* calcite increases with media Sr/Ca mmol/mol. Lopadoliths and muroliths were combined resulting in 64-77 coccoliths for each treatment. The data were fit with a polynomial relationship ($r^2 = 0.92$) and significant differences were determined between all Sr treatments ($p < 0.001$, ANOVA with Dunn's Pairwise Comparison).

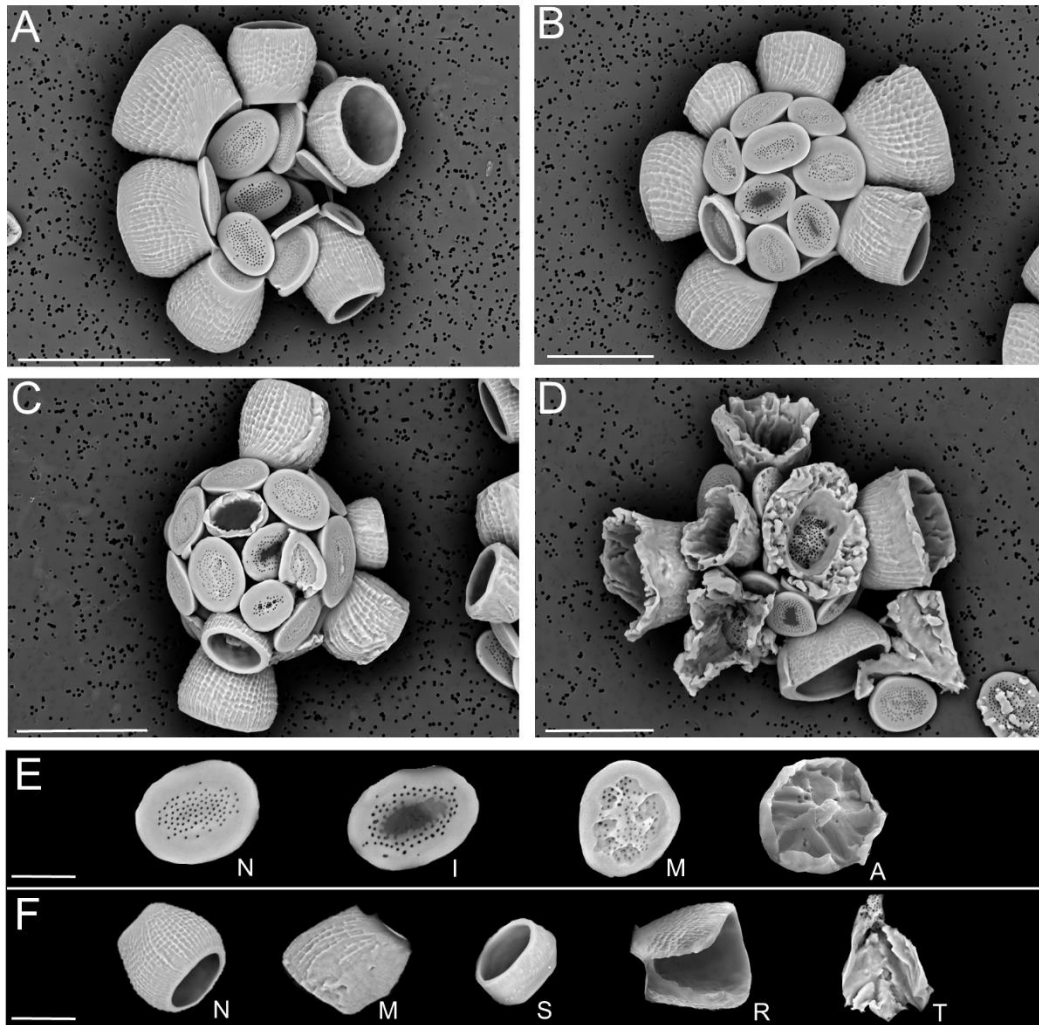


Figure 2. Effect of Sr on *S. apsteinii* coccolith morphology

SEM images acquired with an electron backscatter detector showing the effects of (A) deplete, (B) ambient, and (C,D) high (36 mmol/mol Sr and 72 mmol/mol Sr/Ca respectively) Sr on *S. apsteinii* coccolith morphology. Scale bars represent 20 μm . (E) Examples of murolith morphology scoring categories from left to right: normal, incomplete, malformed, and aberrant. Scale bar represents 5 μm . (F) Examples of lopadolith morphology scoring categories from left to right: normal, malformed (minor malfunctions commonly seen in control cultures), Type S (a short lopadolith with normal morphology), Type R (longitudinal cleavage or sharp edging of lopadolith tip), and Type T (aberrant, completely disorganized calcite).

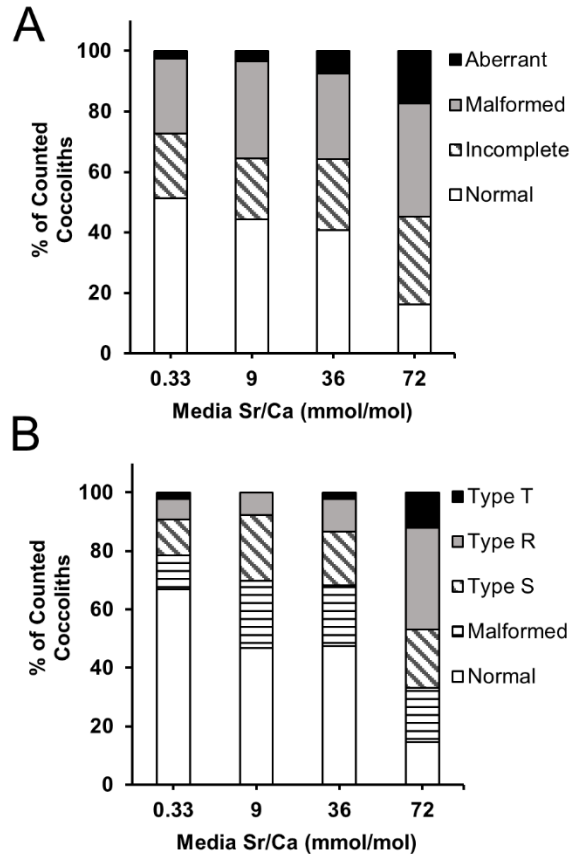


Figure 3. Increased Sr causes an increase in malformed and aberrant coccoliths produced by *S. apsteinii*

(A) Percentage of normal, incomplete, malformed, and aberrant *S. apsteinii* muroliths in coccospheres of cells grown in deplete, ambient, and high Sr (\pm SD). Percentages represent the average for 4 experimental replicates in which 62-85 muroliths from 40 cells were scored for morphology type and divided by the total muroliths counted for that replicate. The frequency of normal muroliths was significantly higher in the 0.33 mmol/mol Sr/Ca compared to all others, while cells grown in the 72 mmol/mol Sr/Ca treatment produced a significantly higher number of aberrant muroliths ($p < 0.001$, ANOVA with Tukey's Pairwise Comparison). (B) Percentage of normal, malformed, Type S, Type R, and Type T *S. apsteinii* lopadoliths (see Fig. 2) from cells grown in deplete, ambient, and high Sr (37-61 lopadoliths from 40 cells from 4 replicate cultures were scored for each Sr treatment \pm SD). The 72 mmol/mol Sr/Ca treatment had a significantly higher number of Type R and Type T lopadoliths ($p < 0.001$ and $p < 0.05$, respectively, ANOVA with Tukey's Pairwise Comparison). The 0.33 mmol/mol Sr/Ca treatment had a significantly higher frequency of normal lopadoliths compared to other Sr treatments ($p < 0.001$, ANOVA with Tukey's Pairwise Comparison). See Table 1 for details.

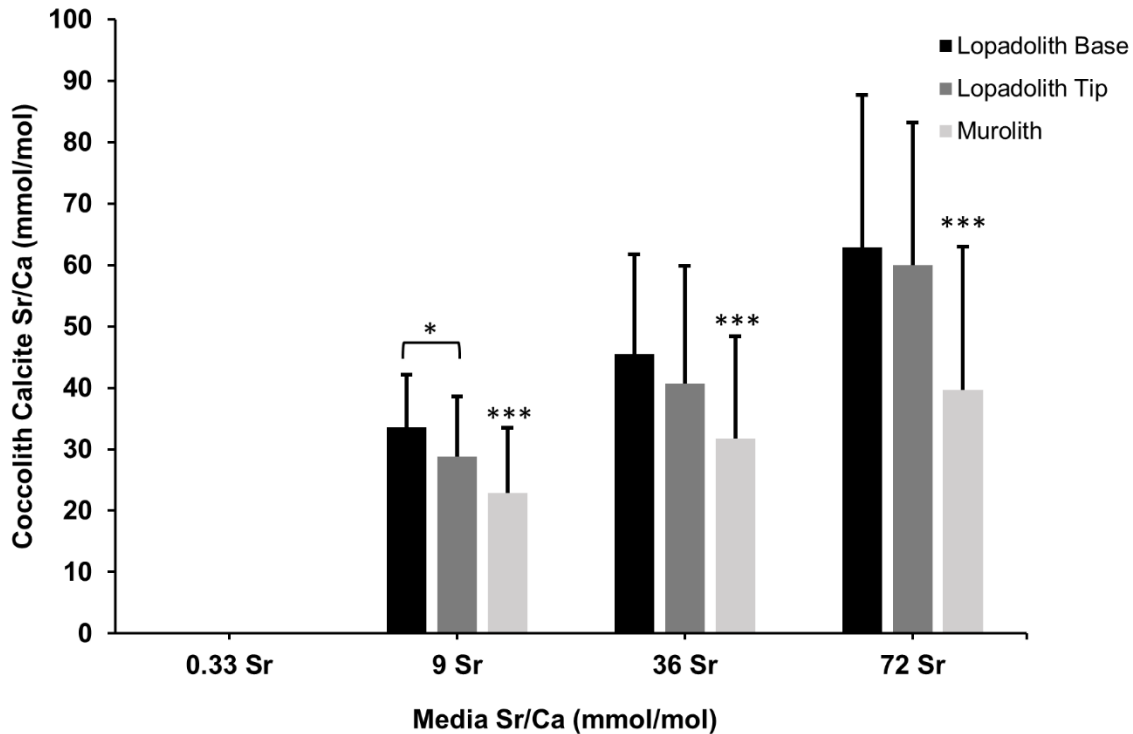


Figure 4. Average Sr/Ca mmol/mol in *S. apsteinii* coccoliths by morphotype in response to increasing media [Sr]

Average calcite Sr/Ca mmol/mol values (\pm SD, $N_{\text{murooliths}} = 63-75$; $N_{\text{lopadolith base}} = 29-36$; $N_{\text{lopadolith tip}} = 29-37$ coccoliths from each experimental treatment) were calculated using Eq. 1 for murooliths and lopadoliths. The Sr/Ca mmol/mol ratio was significantly higher in lopadoliths vs murooliths in the ambient ($p < 0.001$, t-test) and the two enriched Sr treatments ($p < 0.001$, t-test). There was a significantly higher Sr/Ca in the lopadolith base compared to tip in ambient Sr conditions ($p < 0.05$, Student's t-test). There was no significant difference in Sr content between base and tip for the two enriched Sr treatments. The EDS limit of detection (LOD) for Sr was calculated to be 2.29 mmol/mol Sr/Ca. Calculated calcite Sr/Ca values for cells from the 0.33 Sr/Ca mmol/mol treatment were technically at or below LOD for the EDS method and were not further analyzed. See Table 2 for details.

5.0 Citations

- Addadi, L., Joester, D., Nudelman, F. and Weiner, S. (2006) Mollusk shell formation: A source of new concepts for understanding biomineralization processes. *Chem.: Eur. J.* **12**, 981-987.
- Balch, W. M. (2018) The Ecology, Biogeochemistry, and Optical Properties of Coccolithophores. *Annu. Rev. Mar. Sci.* **10**, 71-98.
- Borman, A. H., Dejong, E. W., Huizinga, M., Kok, D. J., Westbroek, P. and Bosch, L. (1982) The role in CaCO₃ crystallization of an acid Ca²⁺ binding polysaccharide associated with coccoliths of *Emiliana-huxleyi*. *Eur. J. Biochem.* **129**, 179-183.
- Bourinet, E., Zamponi, G. W., Stea, A., Soong, T. W., Lewis, B. A., Jones, L. P., Yue, D. T. and Snutch, T. P. (1996) The alpha(1E) calcium channel exhibits permeation properties similar to low-voltage-activated calcium channels. *J. Neurosci.* **16**, 4983-4993.
- Brownlee, C. and Taylor, A. (2004) Calcification in coccolithophores: A cellular perspective. In: *Coccolithophores: from Molecular Processes to Global Impact* (eds H.R. Thierstein and J.R. Young). Springer, Berlin. pp. 31-49.
- Brownlee, C., Wheeler, G. L. and Taylor, A. R. (2015) Coccolithophore biomineralization: New questions, new answers. *Semin. Cell Dev. Biol.* **46**, 11-16.
- Daniels, C. J., Poulton, A. J., Balch, W. M., Maranon, E., Adey, T., Bowler, B. C., Cermenon, P., Charalampopoulou, A., Crawford, D. W., Drapeau, D., Feng, Y. Y., Fernandez, A., Fernandez, E., Fragoso, G. M., Gonzalez, N., Graziano, L. M., Heslop, R., Holligan, P. M., Hopkins, J., Huete-Ortega, M., Hutchins, D. A., Lam, P. J., Lipsen, M. S., Lopez-Sandoval, D. C., Loucaides, S., Marchetti, A., Mayers, K. M. J., Rees, A. P., Sobrino, C., Tynan, E. and Tyrre, T. (2018) A global compilation of coccolithophore calcification rates. *Earth Syst. Sci. Data* **10**, 1859-1876.
- Davis, T. A., Volesky, B. and Mucchi, A. (2003) A review of the biochemistry of heavy metal biosorption by brown algae. *Water Res.* **37**, 4311-4330.
- De Nooijer, L. J., Spero, H. J., Erez, J., Bijma, J. and Reichart, G. J. (2014) Biomineralization in perforate foraminifera. *Earth-Sci. Rev.* **135**, 48-58.
- De Villiers, S. (1999) Seawater strontium and Sr/Ca variability in the Atlantic and Pacific oceans. *Earth Planet. Sc. Lett.* **171**, 623-634.
- Drescher, B., Dillaman, R. M. and Taylor, A. R. (2012) Coccolithogenesis in *Scyphosphaera apsteinii* (Prymnesiophyceae). *J. Phycol.* **48**, 1343-1361.
- Durak, G. M., Brownlee, C., and Wheeler, G. L. (2017) The role of the cytoskeleton in biomineralisation in haptophyte algae. *Sci. Rep.* **7:15409**.

- Fichtinger-Schepman, A. M., Kamerling, J. P., Versluis, C. and Vliegthart, J. F. G. (1981) Structural studies of the methylated, acidic polysaccharide associated with coccoliths of *Emiliania-huxleyi* (Lohmann) Kamptner. *Carbohydr. Res.* **93**, 105-123.
- Flores, J. A., Sierro, F. J., Frances, G., Vazquez, A. and Zamarreno, I. (1997) The last 100,000 years in the western Mediterranean: Sea surface water and frontal dynamics as revealed by coccolithophores. *Mar. Micropaleontol.* **29**, 351-366.
- Fowler, N., Tomas, C., Baden, D., Campbell, L. and Bourdelais, A. (2015) Chemical analysis of *Karenia papilionacea*. *Toxicon.* **101**, 85-91.
- Gafar, N. A., Eyre, B. D. and Kai, G. S. (2019) A comparison of species specific sensitivities to changing light and carbonate chemistry in calcifying marine phytoplankton. *Sci. Rep.* **9:2486**, 1-12.
- Gal, A., Sviben, S., Wirth, R., Schreiber, A., Lassalle-Kaiser, B., Faivre, D. and Scheffel, A. (2017) Trace-element incorporation into intracellular pools uncovers calcium-pathways in a coccolithophore. *Adv. Sci.* **4**, 5.
- Grant, G. T., Morris, E. R., Rees, D. A., Smith, P. J. C. and Thom, D. (1973) Biological interactions between polysaccharides and divalent cations - egg-box model. *FEBS Lett.* **32**, 195-198.
- Grovenor, C. R. M., Smart, K. E., Kilburn, M. R., Shore, B., Dilworth, J. R., Martin, B., Hawes, C. and Rickaby, R. E. M. (2006) Specimen preparation for NanoSIMS analysis of biological materials. *Appl. Surf. Sci.* **252**, 6917-6924.
- Henriksen, K. and Stipp, S. L. S. (2009) Controlling biomineralization: The effect of solution composition on coccolith polysaccharide functionality. *Cryst. Growth Des.* **9**, 2088-2097.
- Henriksen, K., Stipp, S. L. S., Young, J. R. and Marsh, M. E. (2004) Biological control on calcite crystallization: AFM investigation of coccolith polysaccharide function. *Am. Min.* **89**, 1709-1716.
- Hermoso, M. (2014) Coccolith-derived isotopic proxies in palaeoceanography: where geologists need biologists. *Cryptogamie Algol.* **35**, 323-351.
- Hermoso, M., Lefeuvre, B., Minoletti, F. and De Rafelis, M. (2017) Extreme strontium concentrations reveal specific biomineralization pathways in certain coccolithophores with implications for the Sr/Ca paleoproductivity proxy. *Plos One* **12**: e018565, 16.
- Hopkins, J. and Balch, W. M. (2018) A new approach to estimating coccolithophore calcification rates from space. *J. Geophys. Res.-Biogeo.* **123**, 1447-1459.
- Ishii, T., Matsunaga, T., Pellerin, P., O'Neill, M. A., Darvill, A. and Albersheim, P. (1999) The plant cell wall polysaccharide rhamnogalacturonan II self-assembles into a covalently cross-linked dimer. *J. Biol. Chem.* **274**, 13098-13104.

- Kester, D. R., Duedall, I. W., Connors, D. N. and Pytkowicz, R. M. (1967) Preparation of artificial seawater. *Limnol. Oceanogr.* **12**, 176-+.
- Krumhardt, K. M., Lovenduski, N. S., Iglesias-Rodriguez, M. D. and Kleypas, J. A. (2017) Coccolithophore growth and calcification in a changing ocean. *Prog. Oceanogr.* **159**, 276-295.
- Kucerka, N., Papp-Szabo, E., Nieh, M. P., Harroun, T. A., Schooling, S. R., Pencer, J., Nicholson, E. A., Beveridge, T. J. and Katsaras, J. (2008) Effect of cations on the structure of bilayers formed by lipopolysaccharides isolated from *Pseudomonas aeruginosa* PAO1. *J. Phys. Chem. B* **112**, 8057-8062.
- Langer, G., De Nooijer, L. J. and Oetjen, K. (2010) On the role of the cytoskeleton in coccolith morphogenesis: The effect of cytoskeleton inhibitors. *J. Phycol.* **46**, 1252-1256.
- Langer, G., Gussone, N., Nehrke, G., Riebesell, U., Eisenhauer, A., Kuhnert, H., Rost, B., Trimborn, S. and Thoms, S. (2006) Coccolith strontium to calcium ratios in *Emiliania huxleyi*: The dependence on seawater strontium and calcium concentrations. *Limnol. Oceanogr.* **51**, 310-320.
- Littlewood, J. L., Shaw, S., Peacock, C. L., Bots, P., Trivedi, D. and Burke, I. T. (2017) Mechanism of enhanced strontium uptake into calcite via an amorphous calcium carbonate crystallization pathway. *Cryst. Growth Des.* **17**, 1214-1223.
- Mackinder, L., Wheeler, G., Schroeder, D., Riebesell, U. and Brownlee, C. (2010) Molecular mechanisms underlying calcification in coccolithophores. *Geomicrobiol. J.* **27**, 585-595.
- Marsh, M. E. (1994) Polyanion-mediated mineralization - assembly and reorganization of acidic polysaccharides in the golgi system of a coccolithophorid alga during mineral deposition. *Protoplasma* **177**, 108-122.
- Marsh, M. E. (2000) Polyanions in the CaCO₃ mineralization of coccolithophores. In: *Biomineralization: from biology to biotechnology and medical application*. (ed E. Bauerlein). Wiley-VCH, Weinheim. pp. 251-268.
- Marsh, M. E. (2003) Regulation of CaCO₃ formation in coccolithophores. *Comp. Biochem. Phys. B* **136**, 743-754.
- Marsh, M. E., Ridall, A. L., Azadi, P. and Duke, P. J. (2002) Galacturonomannan and Golgi-derived membrane linked to growth and shaping of biogenic calcite. *J. Struct. Biol.* **139**, 39-45.
- Milliman, J. D. (1993) Production and Accumulation of Calcium-Carbonate in the Ocean - Budget of a Nonsteady State. *Global Biogeochem. Cy.* **7**, 927-957.
- Muller, M. N., Krabbenhoft, A., Vollstaedt, H., Brandini, F. P. and Eisenhauer, A. (2018) Stable isotope fractionation of strontium in coccolithophore calcite: Influence of temperature and carbonate chemistry. *Geobiology* **16**, 297-306.

- Outka, D. E. and Williams, D. C. (1971) Sequential Coccolith Morphogenesis in *Hymenomonas carterae*. *J. Protozool.* **18**, 285-297.
- Payne, V. E., Rickaby, R. E. M., Benning, L. G. and Shaw, S. (2008) Calcite crystal growth orientation: implications for trace metal uptake into coccoliths. *Mineral. Mag.* **72**, 269-272.
- Prentice, K., Dunkley Jones, T., Lees, J., Young, J., Bown, P., Langer, G., Fearn, S. and Eimf (2014) Trace metal (Mg/Ca and Sr/Ca) analyses of single coccoliths by Secondary Ion Mass Spectrometry. *Geochim. Cosmochim. Ac.* **146**, 90-106.
- Rickaby, R. E. M., Schrag, D. P., Zondervan, I. and Riebesell, U. (2002) Growth rate dependence of Sr incorporation during calcification of *Emiliana huxleyi*. *Global Biogeochem. Cy.* **16**, 8.
- Rodriguez-Contreras, A., Lv, P., Zhu, J., Kim, H. J. and Yamoah, E. N. (2008) Effects of strontium on the permeation and gating phenotype of calcium channels in hair cells. *J. Neurophysiol.* **100**, 2115-2124.
- Rodriguez-Contreras, A. and Yamoah, E. N. (2003) Effects of permeant ion concentrations on the gating of L-type Ca²⁺ channels in hair cells. *Biophys. J.* **84**, 3457-3469.
- Saavedra-Pellitero, M., Baumann, K. H., Ullermann, J. and Lamy, F. (2017) Marine Isotope Stage 11 in the Pacific sector of the Southern Ocean; a coccolithophore perspective. *Quat. Sci. Rev.* **158**, 1-14.
- Stevenson, E. I., Hermoso, M., Rickaby, R. E. M., Tyler, J. J., Minoletti, F., Parkinson, I. J., Mokadem, F. and Burton, K. W. (2014) Controls on stable strontium isotope fractionation in coccolithophores with implications for the marine Sr cycle. *Geochim. Cosmochim. Ac.* **128**, 225-235.
- Stoll, H. M., Rosenthal, Y. and Falkowski, P. (2002a) Climate proxies from Sr/Ca of coccolith calcite: Calibrations from continuous culture of *Emiliana huxleyi*. *Geochim. Cosmochim. Ac.* **66**, 927-936.
- Stoll, H. M. and Schrag, D. P. (2000) Coccolith Sr/Ca as a new indicator of coccolithophorid calcification and growth rate. *Geochem. Geophys. Geosyst.* **1**, 24.
- Stoll, H. M., Shimizu, N., Archer, D. and Ziveri, P. (2007a) Coccolithophore productivity response to greenhouse event of the Paleocene-Eocene Thermal Maximum. *Earth Planet. Sc. Lett.* **258**, 192-206.
- Stoll, H. M., Ziveri, P., Geisen, M., Probert, I. and Young, J. R. (2002b) Potential and limitations of Sr/Ca ratios in coccolith carbonate: new perspectives from cultures and monospecific samples from sediments. *Philos. T. R. Soc. A* **360**, 719-747.

- Stoll, H. M., Ziveri, P., Shimizu, N., Conte, M. and Theroux, S. (2007b) Relationship between coccolith Sr/Ca ratios and coccolithophore production and export in the Arabian Sea and Sargasso Sea. *Deep-Sea Res. Pt. II* **54**, 581-600.
- Sucheras-Marx, B., Giraud, F., Simionovici, A., Daniel, I. and Tucoulou, R. (2016) Perspectives on heterococcolith geochemical proxies based on high-resolution X-ray fluorescence mapping. *Geobiology* **14**, 390-403.
- Sun, S. Y., Liu, M. X., Nie, X. Q., Dong, F. Q., Hu, W. Y., Tan, D. Y. and Huo, T. T. (2018) A synergetic biomineralization strategy for immobilizing strontium during calcification of the coccolithophore *Emiliana huxleyi*. *Environ. Sci. Pollut. R.* **25**, 22446-22454.
- Taylor, A. R., Brownlee, C., Wheeler, G. and Annual, R. (2017) Coccolithophore Cell Biology: Chalking Up Progress. *Annu. Rev. Mar. Sci.* **9**, 283-310.
- Walker, C. E., Heath, S., Salmon, D. L., Smirnoff, N., Langer, G., Taylor, A. R., Brownlee, C. and Wheeler, G. L. (2018a) An Extracellular Polysaccharide-Rich Organic Layer Contributes to Organization of the Cocosphere in Coccolithophores. *Front. Mar. Sci.* **5**, 12.
- Walker, C. E., Taylor, A. R., Langer, G., Durak, G. M., Heath, S., Probert, I., Tyrrell, T., Brownlee, C. and Wheeler, G. L. (2018b) The requirement for calcification differs between ecologically important coccolithophore species. *New Phytol.* **220**, 147-162.
- Wasylenki, L. E., Dove, P. M., Wilson, D. S. and De Yoreo, J. J. (2005) Nanoscale effects of strontium on calcite growth: An in situ AFM study in the absence of vital effects. *Geochim. Cosmochim. Ac.* **69**, 3017-3027.
- Westbroek, P., Dejong, E. W., Vanderwal, P., Borman, A. H., Devrind, J. P. M., Kok, D., Debruijn, W. C. and Parker, S. B. (1984) Mechanism of calcification in the marine alga *Emiliana-huxleyi*. *Philos. Trans. R. Soc. Lond. B Biol. Sci.* **304**, 435-&.
- Woodward, C. and Davidson, E. A. (1968) Structure-function relationships of protein polysaccharide complexes - specific ion-binding properties. *Proc. Natl. Acad. Sci. U.S.A.* **60**, 201-205.
- Young, J. R., Davis, S. A., Bown, P. R. and Mann, S. (1999) Coccolith ultrastructure and biomineralisation. *J. Struct. Biol.* **126**, 195-215.
- Young, J. R., Poulton, A. J. and Tyrrell, T. (2014) Morphology of *Emiliana huxleyi* coccoliths on the northwestern European shelf - is there an influence of carbonate chemistry? *Biogeosciences* **11**, 4771-4782.